# Identifying Sequential Substrate Binding at the Single-Molecule Level by Enzyme Mechanical Stabilization
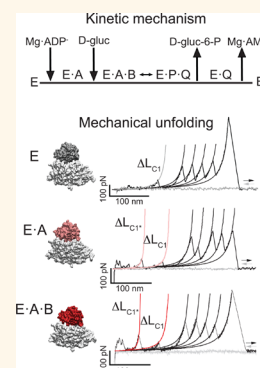
Jaime Andrés Rivas-Pardo,[*,†,‡] Jorge Alegre-Cebollada,[†] César A. Ramírez-Sarmiento,[‡] Julio M. Fernandez,[*,†] and Victoria Guixé[*,‡]

[†]Department of Biological Sciences, Columbia University, Northwest Corner Building, 550 West 120 Street, New York, New York 10027, United States and [‡]Laboratorio de Bioquímica y Biología Molecular, Departamento de Biología, Facultad de Ciencias, Universidad de Chile, Las Palmeras 3425, Casilla 653, Santiago, Chile

**ABSTRACT** Enzyme—substrate binding is a dynamic process intimately coupled to protein structural changes, which in turn changes the unfolding energy landscape. By the use of single-molecule force spectroscopy (SMFS), we characterize the open-to-closed conformational transition experienced by the hyperthermophilic adenine diphosphate (ADP)-dependent glucokinase from *Thermococcus litoralis* triggered by the sequential binding of substrates. In the absence of substrates, the mechanical unfolding of TlGK shows an intermediate 1, which is stabilized in the presence of $Mg \cdot ADP^-$, the first substrate to bind to the enzyme. However, in the presence of this substrate, an additional unfolding event is observed, intermediate 1*. Finally, in the presence of both substrates, the unfolding force of intermediates 1 and 1* increases as a consequence of the domain closure. These results show that SMFS can be used as a powerful experimental tool to investigate binding mechanisms of different enzymes with more than one ligand, expanding the repertoire of protocols traditionally used in enzymology.

**KEYWORDS:** single-molecule force spectroscopy · force—extension · mechanical intermediate · mechanical clamp · substrate stabilization

I n recent years, evidence has accumulated to demonstrate that the binding of substrates triggers a conformational rearrangement of enzyme structure.[1−4] In many cases, these conformational changes alternate through structural states that favor substrate binding, release of products, or protection of the transition state from attack by solvent molecules.[4−7] In addition, these conformational changes are related to the sequential binding of substrates.[2,8−10] However, it is not easy to determine the presence of ligand binding or the order in which binding occurs when more than one substrate is required. Since the seminal work of Cleland, determination of the kinetic mechanism of enzymes has been achieved using methods that involve enzyme activity assays in the presence of different concentrations of substrates, products, and inhibitors.[11−15] Although this approach is well-defined, in many cases, there are practical barriers that prevent its realization, such as substrate inhibition, the absence of an appropriate coupled assay, and compound solubility, among others.[16−19] The mechanical stabilization of enzymes and proteins by ligand binding is a phenomenon that has been explored previously.[20−27] Substrates and ligands affect the energy landscape of different structural segments of a protein and, in many cases, increase the mechanical stability of the protein as a consequence of the favorable binding interactions.[28−30]

The adenine diphosphate (ADP)-dependent glucokinase from *Thermococcus litoralis* (TlGK) represents a suitable model to explore the mechanical stabilization of enzymes as a signature of the effective binding of substrates and inhibitors. TlGK exhibits sequential binding of its substrates, which correlates with well-defined structural transitions that occur both in solution and in crystalline states.[31] TlGK is a hyperthermophilic enzyme that catalyzes the phosphate transfer from $Mg \cdot ADP^-$ to D-glucose, the first reaction of a modified version of the Embden—Meyerhof metabolic pathway

* Address correspondence to
jar2228@columbia.edu,
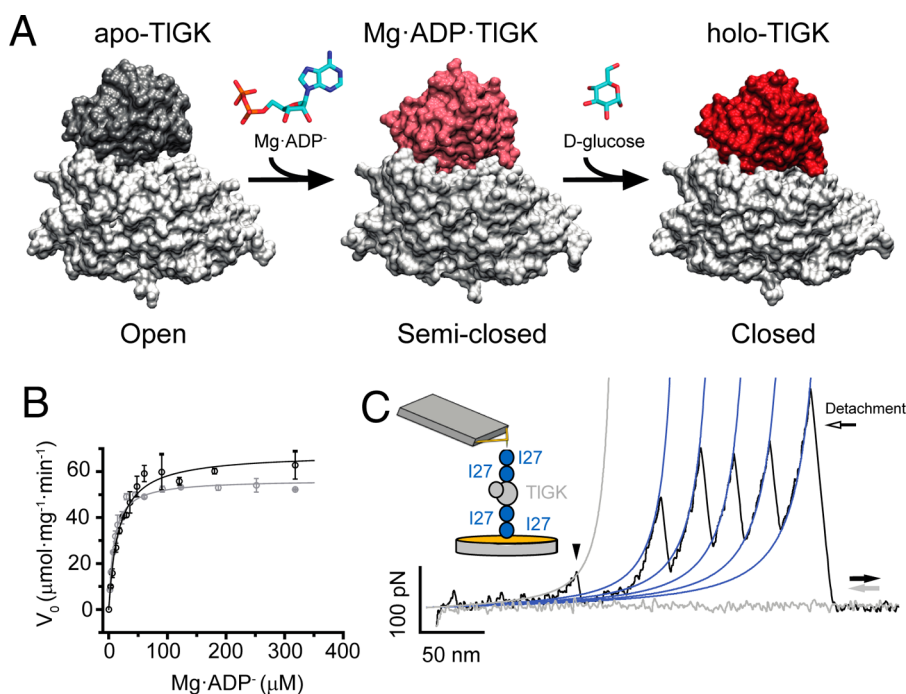jfernandez@columbia.edu,
vguixe@uchile.cl.

Figure 1. Single-molecule force spectroscopy of TlGK. (A) Crystal structures of TlGK. Substrate binding leads to conformational rearrangements, triggering the closure of domains. The large domain is colored in light gray for all conditions, whereas the small domains are shown in gray in the absence of substrate, pink in the presence of $Mg \cdot ADP^{-}$, and red in the presence of both substrates. The binding site is located in the cleft formed between both domains. (B) Activity of the enzyme TlGK in the polyprotein. $Mg \cdot ADP^{-}$ saturation curves for soluble monomer TlGK (gray circles) and $(I27)_2$-TlGK-$(I27)_2$ (black circles). Both curves were fitted using the Michaelis–Menten model (eq 1). Table 1 summarizes the kinetic constant for the phosphate transfer reaction. (C) Representative trace for the mechanical unfolding of $(I27)_2$-TlGK-$(I27)_2$. Inset: Schematic representation of the polyprotein under mechanical tension. I27 modules are represented in blue, and TlGK is in gray. The arrowhead indicates the main mechanical intermediate present in TlGK. Four consecutive peaks are detected, belonging to the unfolding of the I27 modules. The last peak at the end of each trace corresponds to the detachment of the protein from the cantilever or the gold surface. Fits correspond to the worm-like chain model.[53,54]

present in archaea.[32] The structure of TlGK features a large Rossmann-like domain and a small $\alpha/\beta$ domain that emerges as a topological discontinuity,[33,34] with the active site lying between both domains (Figure 1A). Substrate binding in TlGK has been proposed to follow a sequentially ordered kinetic mechanism: $Mg \cdot ADP^{-}$ is the first substrate to bind to the enzyme, whereas D-glucose binds only when the $TlGK \cdot Mg \cdot ADP^{-}$ complex is already formed. Structural analysis reveals a conformational change from an open to a semiclosed state after nucleotide binding, while binding of D-glucose to this binary complex induces a fully closed conformation (Figure 1A).[31]

Here we develop a single-molecule strategy to assess the sequential binding of substrates as an increase in the mechanical stability of TlGK, which is widely applicable to enzymes whose mechanical stability changes with the binding of substrates. Compared to more conventional methods, this strategy requires only a low concentration of enzyme, substrates, and inhibitors and is independent of enzyme activity, which circumvents many of the problems associated with the traditional approaches employed in enzymology (kinetic assays) and provides a direct measurement of the protein–ligand interaction. As such, it could be useful

in drug design efforts since this strategy allows for the evaluation of the binding of inhibitors that modulate enzyme activity.

## RESULTS

**Activity of TlGK in the Polyprotein.** In order to manipulate the protein at the single-molecule level, TlGK was engineered into a polyprotein construct, with two I27 domains from human cardiac titin flanking both ends of the enzyme. The I27 domain from titin has been extensively studied, and its mechanical properties can be used as a "fingerprint" to identify unambiguously the manipulation of a single molecule.[23,35,36] To confirm TlGK functionality in the $(I27)_2$-TlGK-$(I27)_2$ polyprotein, kinetic parameters for the phosphate transfer reaction were measured and compared with the values obtained for the soluble monomer. For both enzymes, saturation curves for $Mg \cdot ADP^{-}$ and D-glucose are very similar, yielding almost identical values for $K_M$ and $V_{max}$ (Figure 1B and Table 1). These results demonstrate that TlGK in the polyprotein construct is capable of binding substrates and catalyzing phosphoryl transfer with unaltered kinetic constants.

**Mechanical Unfolding of Apo- and Holo-enzyme.** The polyprotein was pulled using a constant velocity protocol

($400 \text{ nm} \cdot \text{s}^{-1}$). Figure 1C shows a characteristic force–extension trace corresponding to the unfolding of $(I27)_2$-TlGK-$(I27)_2$. We considered traces that show at least three unfolding events of the I27 module, in addition to the detachment event. The first unfolding event occurs at low force and after a large extension of the polyprotein (Figure 1C, arrowhead), while the next

events are essentially identical because they share the same extension and force. These results indicate that the first mechanical event corresponds to TlGK, mechanical intermediate 1, whereas the others belong to the unfolding of I27 modules.

For every trace recorded, four characteristic lengths were measured: full extension of the polypeptide (final extension, $L_f$), extension before I27 module unfolding (initial extension, $L_i$), extension of the mechanical intermediate present in TlGK, and finally, extension of every I27 module (Figure 2A and Table 2). The average value for $L_f$ is $314 \pm 6$ nm (Figure 2B), whereas the value for $L_i$ is $193 \pm 7$ nm (Figure 2C). Assuming a length per residue of 0.4 nm,[37] the fully extended construct $(I27)_2$-TlGK-$(I27)_2$ should reach 339 nm (845 residues; see Methods), whereas the extended TlGK + linkers (489 residues; see Methods) should be 196 nm. Thus, our values for $L_f$ and $L_i$ are in very good agreement with the theoretical extension for the fully extended polyprotein and TlGK, respectively. The mechanical intermediate 1, which is present in the unfolding of

**TABLE 1. Enzyme Kinetic Parameters for ADP-Dependent TlGK**[a]

| | TlGK | | $(I27)_2$-TlGK-$(I27)_2$ | |
|---|---|---|---|---|
| | $K_M$ ($\mu$M) | $V_{MAX}^{\ddagger}$ ($\mu$mol·mg$^{-1}$·min$^{-1}$) | $K_M$ ($\mu$M) | $V_{MAX}^{\ddagger}$ ($\mu$mol·mg$^{-1}$·min$^{-1}$) |
| Mg·ADP$^-$ | $8.4 \pm 0.7$ | $57 \pm 1$ | $16 \pm 2$ | $67 \pm 2$ |
| D-glucose | $219 \pm 2$ | $57 \pm 1$ | $300 \pm 5$ | $67 \pm 2$ |

[a] Values obtained from fitting the data to the Michaelis–Menten model (eq 1). Values are given as mean $\pm$ standard deviation of the fit from three independent measurements. $V_{MAX}^{\ddagger}$ corresponds to the average value between measurements with Mg·ADP$^-$ and D-glucose as variable substrates.
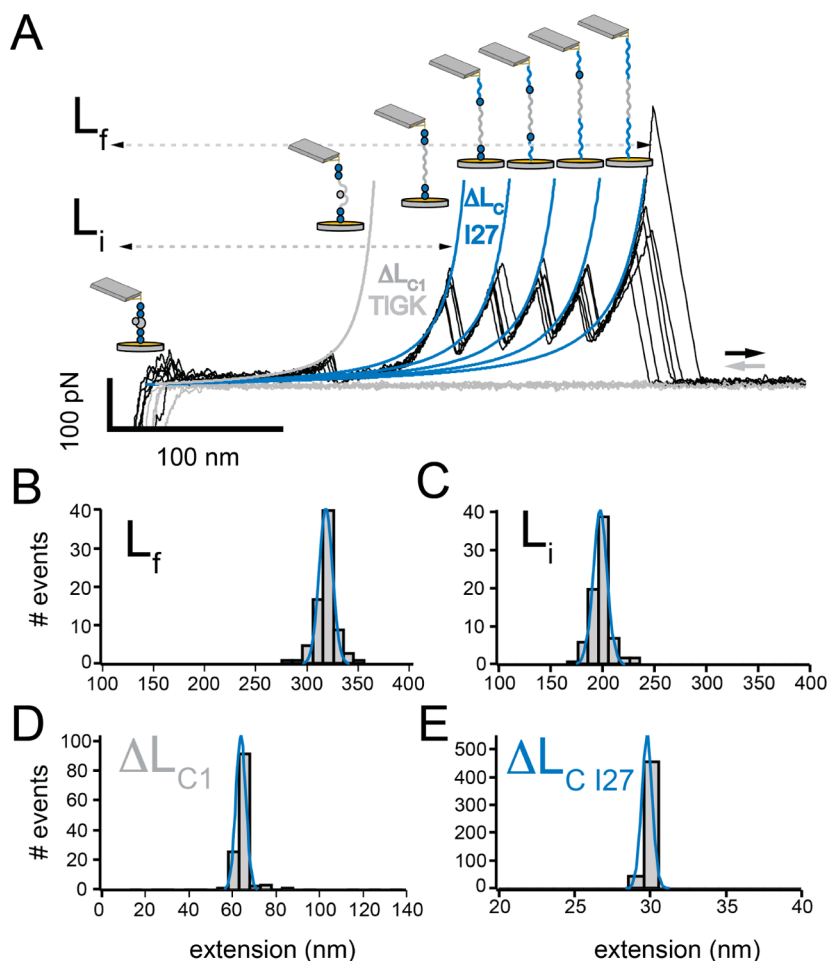


**Figure 2. Fingerprint of the polyprotein $(I27)_2$-TlGK-$(I27)_2$.** (A) Total lengths measured in the force–extension traces. Final extension ($L_f$) and initial extension of the polyprotein ($L_i$) correspond to the length where the polyprotein is totally unfolded and the extension of the polyprotein before the mechanical unfolding of the I27 modules, respectively. Fits correspond to the worm-like chain model.[53,54] (B,C) Histograms of $L_f$ and $L_i$, respectively. For $L_f$ and $L_i$, only traces with four I27 events were considered ($n = 77$). (D,E) Contour length increment for the mechanical intermediate present in the TlGK ($n = 139$) and I27 (511), respectively. Table 2 summarizes all the extensions calculated for the polyprotein.

**TABLE 2. Mean Extensions for the Unfolding of (I27)$_2$-TIGK-(I27)$_2$[a]**

|  | $L_f$ (nm) | $L_i$ (nm) | I27 $\Delta L_{C1}$ (nm) | TIGK $\Delta L_{C1}$ (nm) | TIGK pL (nm) | $n$ |
|---|---|---|---|---|---|---|
| apo-enzyme | 314 ± 6 | 193 ± 7 | 29.3 ± 0.4 | 61 ± 2 | 0.58 ± 0.11 | 139 (77) |
| D-glucose | 304 ± 6 | 181 ± 8 | 29.0 ± 0.5 | 59 ± 3 | 0.54 ± 0.17 | 88 (51) |
| Mg·ADP$^-$ | 328 ± 14 | 207 ± 16 | 29.5 ± 0.4 | 61 ± 3 | 0.48 ± 0.18 | 71 (41) |
| holo-enzyme | 315 ± 8 | 195 ± 8 | 29.7 ± 0.5 | 62 ± 4 | 0.44 ± 0.13 | 82 (50) |
| Mg·GDP$^-$ | 323 ± 15 | 196 ± 13 | 29.6 ± 0.5 | 59 ± 3 | 0.46 ± 0.12 | 64 (48) |
| Mg·ADP-GLC | 309 ± 14 | 186 ± 6 | 29.36 ± 0.03 | 60 ± 4 | 0.43 ± 0.1 | 107 (77) |

[a] Distances were calculated using the worm-like chain model.[53,54] $L_f$ and $L_i$ consider only traces with four I27 unfolding events; pL is the persistence length fitted from the worm-like chain model; $n$ corresponds to the total number of unfolding events. The numbers in parentheses correspond to traces with four I27 unfolding events used for $L_f$ and $L_i$. The extension values reported correspond to the mean value ± standard deviation from Gaussian fits (Figure 2).
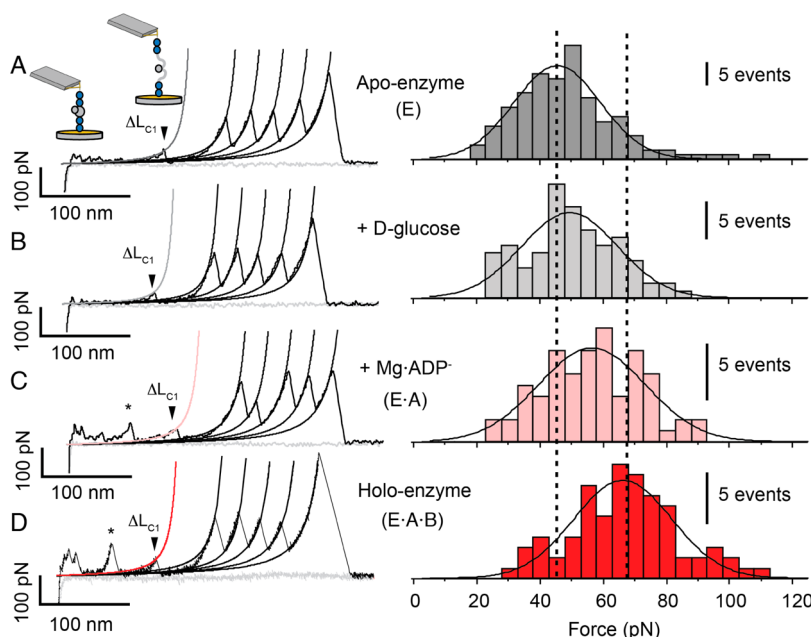


**Figure 3. Mechanical stabilization of intermediate 1. (A−D) Left: Examples of force−extension traces under the different conditions explored: absence of substrates, presence of D-glucose, Mg·ADP$^-$, and holo-enzyme, respectively. Arrowhead shows the mechanical intermediate present in the TIGK. Note that traces in C and D show an extra mechanical intermediate (asterisks). Fits in the traces correspond to the worm-like chain model.[53,54] The fits are shown in gray, light gray, pink, and red, in accordance with the experimental condition. (A−D) Right: Histograms of the unfolding forces for $\Delta L_{C1}$ under the same conditions. Bar shows the number of events. Solid black line corresponds to a Gaussian fit to the different conditions: apo-enzyme, D-glucose, Mg·ADP$^-$, and holo-enzyme. Dotted black lines indicate the transition for the unfolding force value between the apo and holo-enzyme. Table 3 and Supporting Information Table S1 summarize the unfolding forces for every experimental condition.**

TIGK, has an average extension of the contour length increment ($\Delta L_{C1}$) of 61 ± 2 nm (Figure 2D), suggesting that ∼153 amino acids are involved in this mechanical intermediate. Finally, the contour length increment for the I27 module ($\Delta L_{CI27}$) is 29 ± 1 nm (Figure 2E), in agreement with previously published values.[38,39]

Thus, we measured the effect of the substrates on the mechanical unfolding of TIGK. The presence of the substrates produces no difference in the extension of $L_i$, $L_f$, or $\Delta L_{C1}$ (Table 2). However, the substrates trigger an increase in the unfolding forces for the mechanical intermediate 1. We observed that this increase in the unfolding force is in accordance with the particular binding of the substrates. When the substrate Mg·ADP$^-$ was assayed, the unfolding force increases from 43 ± 14 pN in the apo-enzyme to 54 ± 17 pN (Figure 3A,C and Table 3), whereas the unfolding force

**TABLE 3. Mean Unfolding Forces of $\Delta L_{C1}$ and $\Delta L_{CI27}$[a]**

|  | TIGK | | | I27 | | |
|---|---|---|---|---|---|---|
|  | force (pN) | $n$ | $P$ | force (pN) | $n$ | $P$ |
| apo-enzyme | 43 ± 14 | 139 |  | 213 ± 24 | 511 |  |
| D-glucose | 47 ± 15 | 88 | >0.05 | 214 ± 29 | 315 | >0.05 |
| Mg·ADP$^-$ | 54 ± 17 | 71 | <0.05 | 215 ± 24 | 259 | >0.05 |
| holo-enzyme | 64 ± 15 | 82 | <0.001 | 213 ± 23 | 297 | >0.05 |
| Mg·GDP$^-$ | 54 ± 15 | 64 | <0.05 | 212 ± 23 | 238 | >0.05 |
| Mg·ADP-GLC | 60 ± 18 | 107 | <0.001 | 227 ± 26 | 401 | >0.05 |

[a] The forces reported in the table are the mean value ± standard deviation from the Gaussian fits (Figure 3). Statistical analysis was made using one-way Anova. $P$ values in the table are considering apo-condition as reference.

in the presence of D-glucose reaches only 47 ± 15 pN, which is not significantly different from the value
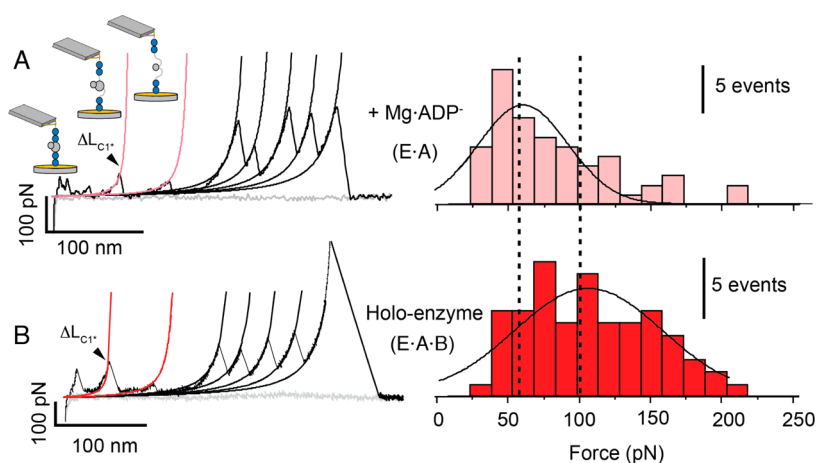
**Figure 4.** Mechanical intermediate 1* in the E·A and E·A·B complex. (A,B) Left: Force−extension traces of the unfolding in the presence of only Mg·ADP⁻ and of both substrates, showing the additional mechanical intermediate 1* (arrowheads). Fits in the traces correspond to the worm-like chain model.[53,54] (A,B) Right: Histograms of the unfolding forces for $\Delta L_{C1*}$ in the presence of Mg·ADP⁻ and holo-enzyme. Bar shows the number of events. Solid black line corresponds to a Gaussian fit. Dotted black lines indicate the transition of the unfolding force value between the apo- and holo-enzyme. The unfolding forces and extension for $\Delta L_{C1*}$ are summarized in Table 4 and Supporting Information Table S1.

**TABLE 4. Mean Extensions and Unfolding Forces of $\Delta L_{C1*}{}^{a}$**

|  | extension (nm) | pL (nm) | force (pN) | P | n | % |
|---|---|---|---|---|---|---|
| holo-enzyme | 66 ± 22 | 0.5 ± 0.2 | 93 ± 52 |  | 72 | 87 |
| Mg·ADP⁻ | 68 ± 34 | 0.5 ± 0.2 | 53 ± 31 | <0.01 | 59 | 83 |
| Mg·GDP⁻ | 68 ± 9 | 0.57 ± 0.09 | 47 ± 16 | <0.001 | 44 | 69 |
| Mg·ADP-GLC | 67 ± 21 | 0.4 ± 0.1 | 49 ± 15 | <0.001 | 92 | 86 |

$^{a}$ The forces reported in the table are the mean value ± standard deviation from the Gaussian fits (Figures 4 and 5); pL is the persistence length fitted from the worm-like chain model.[53,54] Statistical analysis was made using one-way Anova. P values in the table consider the holo-enzyme as reference.

obtained for the apo-enzyme (Figure 3A,B and Table 3). These results suggest that D-glucose does not bind to the enzyme in the absence of the Mg·ADP⁻, which is in agreement with previous kinetic experiments.[31] Finally, we explored the effect on the mechanical intermediate 1 when the ternary complex is mimicked by the use of the nonhydrolyzable ADP analogue, ADPβS. In the TlGK·Mg·ADPβS-D-glucose complex, holo-enzyme, the unfolding force increased to 64 ± 15 pN (Figure 3A,D and Table 3), 20 pN more than the value observed in the apo-enzyme. Statistical analysis suggests that it is possible to identify three different mechanical states: (i) enzyme in the absence of substrate, apo-enzyme (E), (ii) enzyme in complex with Mg·ADP⁻ (E·A), and (iii) the enzyme with both substrates bound, holo-enzyme (E·A·B). All the unfolding forces are summarized in Table 3 and Supporting Information Table S1.

An additional mechanical intermediate was apparent in experiments where the enzyme was pulled as the E·A and E·A·B complexes (asterisk in Figure 3 and Figure 4). This event is less populated in the apo-enzyme because we calculated that less than 20% of unfolding events visit this intermediate 1*. While for

the E·A and E·A·B conditions, 83 and 87% of the traces visit the intermediate 1*, respectively. In the E·A complex, the contour length for this intermediate, $\Delta L_{C1*}$, is 68 ± 34 nm and the mechanical unfolding force is 52 ± 31 pN (Figure 4A and Table 4), whereas in the holo-enzyme, the $\Delta L_{C1*}$ is 66 ± 22 nm and the unfolding force reaches a value of 93 ± 52 pN (Figure 4A,B and Table 4). The difference in force between these two conditions is statistically significant; therefore, by using $\Delta L_{C1*}$, it is also possible to distinguish the E·A complex from the ternary E·A·B complex (Table 4 and Supporting Information Table S1).

Finally, to confirm the specificity of the stabilization effect achieved by substrates in TlGK, we used the unfolding forces of the I27 module as a control. As shown in Supporting Information Figure S1, the force necessary to unfold I27 remains close to ~200 pN, regardless of the substrate present in the solution (Table 3 and Supporting Information Table S1). Thus, sequential binding of substrates is specific and affects only the unfolding forces of TlGK and not the I27 modules.

**Inhibitors Also Change the Mechanical Stability of TlGK.** Modulation of enzyme activity is a key aspect of proper cellular function. This can be achieved by inhibitory compounds that are structurally related to natural substrates but unable to support catalysis or by allosteric effectors. In order to evaluate if mechanical stabilization is also exerted by TlGK inhibitors, we measured the mechanical stability of TlGK in the presence of Mg·GDP⁻, an analogue of Mg·ADP⁻, and Mg·adenosine-5′-diphosphoglucose (Mg·ADP-GLC), which mimics ternary complex formation. In the presence of inhibitors, we distinguish the same mechanical intermediates 1 and 1*, with no difference in the extension $\Delta L_{C1}$ and $\Delta L_{C1*}$ (Table 2). However, both
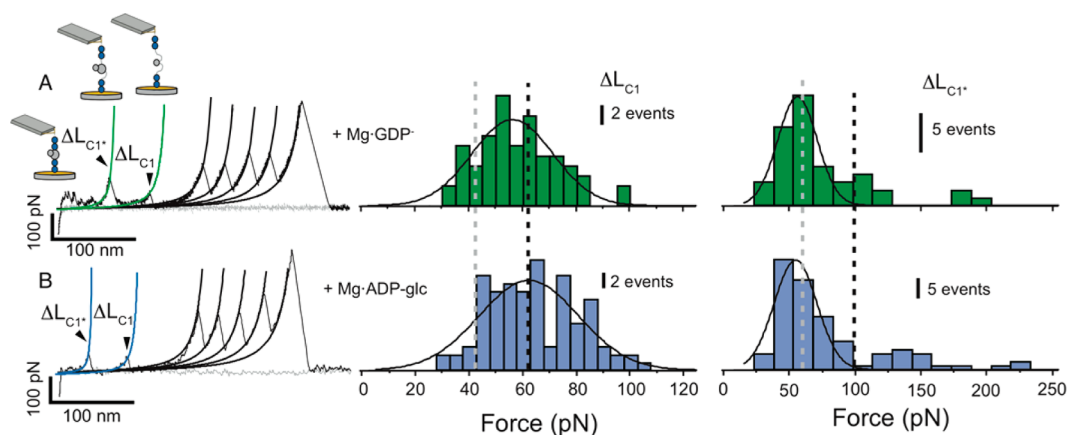
**Figure 5. Mechanical stabilization by inhibitors of TlGK. (A,B) Left: Force−extension traces of the unfolding in the presence of Mg·GDP⁻ and Mg·ADP-GLC showing both mechanical intermediates $\Delta L_{C1}$ and $\Delta L_{C1*}$ (arrowheads). Fits in the traces correspond to the worm-like chain model.[53,54] (A,B) Middle and right: Histograms of the unfolding forces for $\Delta L_{C1}$ and $\Delta L_{C1*}$, respectively. Bars in the histograms correspond to the number of events. The unfolding forces and extension for the mechanical intermediates $\Delta L_{C1}$ and $\Delta L_{C1*}$ are summarized in Table 4 and Supporting Information Table S1.**

inhibitors trigger a mechanical stabilization of the intermediates. Mg·GDP⁻ increases the unfolding force for the intermediate 1 to 54 ± 15 pN, whereas Mg·ADP-GLC increases the unfolding force to 60 ± 18 pN, in good agreement with the values obtained for Mg·ADP⁻ binding (Figure 5, Table 3, and Supporting Information Table S1). These results in the presence of the inhibitors show a statistically significant difference with respect to the apo-enzyme, triggering a stabilization equivalent to the one detected in the presence of Mg·ADP⁻ (Table 4 and Supporting Information Table S1). On the other hand, the mean value of the unfolding force for the mechanical intermediate 1* is 47 ± 16 pN in the presence of Mg·GDP⁻ and 49 ± 15 pN in the presence of Mg·ADP-GLC (Figure 5, Table 4, and Supporting Information Table S1). In this case, statistical analysis indicated that both inhibitors do not stabilize the intermediate 1* as occurs in the E·A·B complex; rather, the mechanical behavior is comparable to the binding of Mg·ADP⁻ (Table 4 and Supporting Information Table S1).

## DISCUSSION

Determining the order of substrate binding in enzymes with more than one substrate is critical to understand the individual steps involved in catalysis and is an essential information for drug design. Traditional methods involve spectrophotometric techniques, which usually require large amounts of enzyme, substrates, and inhibitors. Additionally, for many enzymes, a direct method to detect product formation is not available, in which case, coupled enzyme assays are extensively used. Also, there are several examples where it is not possible to monitor the enzymatic activity in real time, requiring the use of complex and sophisticated techniques.[40,41] In the case of TlGK, enzyme kinetic studies indicated a sequentially ordered mechanism where Mg·ADP⁻ is the first substrate to bind to the enzyme (E·A complex), and

D-glucose binds to the E·A complex, leading to ternary complex formation (E·A·B). These binding events are accompanied by successive conformational rearrangements. Small-angle X-ray scattering studies indicate that the complex E·A closes slightly, and only after the binding of the D-glucose, is the domain closure complete (Figure 1A).[31] Here we used mechanical perturbation of TlGK at the single-molecule level to capture these different protein conformations. Force−extension experiments indicate the presence of two mechanical intermediates, $\Delta L_{C1}$ with an extension of 60 nm and $\Delta L_{C1*}$ with 66 nm, both sensitive to the binding of substrates (Tables 2−4). In the presence of both substrates (holo-enzyme), an additional 20 pN is needed to reach the unfolded state of the intermediate $\Delta L_{C1}$. This change represents an increase of 50% in the force required to unfold the mechanical intermediate with respect to the apo-form. Furthermore, the intermediate 1* allows the clear distinction between complexes, with a 44 pN difference between E·A and the E·A·B ternary complex. Additionally, the lack of change in the unfolding forces obtained in the presence of D-glucose suggests nonbinding of the sugar in the absence of Mg·ADP⁻. However, binding without any change in the unfolding force has been reported before,[26] thus we cannot completely rule out this possibility. In the case of TlGK, a sequentially ordered kinetic mechanism has been proposed, where D-glucose is bound to the enzyme only after the complex TlGK·Mg·ADP⁻ is formed.[31] Additionally, we have performed binding experiments that suggest that D-glucose binding occurs only in the presence of nucleotide (Supporting Information Figure S2). Thus, the lack of change in force in the presence of D-glucose could be understood as the absence of D-glucose binding. Therefore, our results fully support the kinetic mechanism for the enzyme: binding of the Mg·ADP⁻ complex followed by the binding of D-glucose. In summary, our assay is able to detect at the single-molecule level every state

generated in solution during the catalytic reaction cycle (E, E·A, and E·A·B).

During the past decades, several models have emerged to explain the relationship between conformational changes and ligand binding. The *induced fit model*, originally raised by Koshland,[42] proposes that the structure of the enzyme changes by the binding of ligands, whereas the *conformational selection model* states that in solution the enzyme exists as an ensemble of conformations and only a fraction is able to bind ligands.[43,44] Based on crystal structures, Sullivan and Holyoak demonstrated that the phosphoenolpyruvate carboxykinase operates through an induced fit mechanism, as well as other enzymes with lid-gated active sites.[7] For example, TlGK is an $\alpha/\beta$ protein with two domains, where the small domains work as a lid on top of the active site (Supporting Information Figure S3).[34] If the enzyme reaches the closed conformation, there is not enough space for the substrates to access the active site, suggesting that conformational selection is not a plausible option. Our single-molecule experiments are able to distinguish between apo- and holo-forms (Figures 3 and 4), signatures of the open and closed conformations, respectively. These results could suggest that TlGK operates through an induced fit mechanism, where Mg·ADP⁻ and D-glucose trigger the transition to the closed conformation. Prior work from our group based on crystal structures in the absence and presence of ligands and on the kinetic mechanism of TlGK also pointed out the induced fit as the most probable mechanism.[31]

Additionally, our assay was also able to capture binding of inhibitors. The TlGK·Mg·GDP⁻ complex triggers a stabilization effect similar to the one observed in the presence of Mg·ADP⁻, in agreement with the competitive inhibition exerted by the analogue with respect to this substrate. On the other hand, the Mg·ADP-GLC ternary complex analogue also exerts a mechanical stabilization, but in this case, the stabilization is not equivalent to that found in the holo-enzyme; rather, it is similar to the effect observed in the presence of Mg·ADP⁻ (Figure 5 and Table 4). It is probable that the different positions of the D-glucose hydroxyls in this analogue impair the proper structural rearrangements related to catalysis in the enzyme. These results suggest that binding of Mg·GDP⁻ or Mg·ADP-GLC precludes the formation of the E·A complex and induces conformational changes equivalent to the ones observed for the substrate Mg·ADP⁻, although they are not able to sustain catalysis.

Mechanical stabilization by ligands at the single-molecule level has been observed in other proteins. The force required to unfold the maltose binding protein can be modulated by the introduction of maltose in the solution,[20] which also has consequences on the unfolding pathway.[45] A similar effect was reported in titin kinase, where the introduction of

ATP into the solution modifies the number of mechanical intermediates present in force—extension curves.[46] A very sophisticated example of mechanical unfolding modulation is observed in protein G and the Fc fragment of IgG.[47] Adding the Fc fragment at concentrations in the micromolar range increases the unfolding force from 100 to 200 pN. Furthermore, the change is concentration-dependent, thus making it possible to determine the dissociation constant for the protein G—Fc complex. However, to the best of our knowledge, TlGK is the first example of a sequential mechanical modulation where protein stabilization follows the binding of substrates in accordance with the kinetic mechanism.

Moreover, TlGK unfolding follows a pathway with more than one intermediate that can be modified by the presence of substrates. In the apo-form, only 20% of the unfolding events present both mechanical intermediates. However, when Mg·ADP⁻ or Mg·ADP$\beta$S·D-GLC is added to the solution, more than 80% of the unfolding events show both mechanical intermediates. These results would suggest that binding of substrates modifies the unfolding pathway, from one to two mechanical intermediates. Examples of proteins with more than one mechanical intermediate have been described before. Leucine binding protein unfolds following a two-state pathway in the presence of leucine, but in the absence of substrate, the unfolding becomes more complex and a multiple three-state pathway predominates.[30] Also, the phosphatidyl-*myo*-inositol mannosyltransferase A shows a heterogeneous unfolding pathway with multiple steps.[48] In our case, TlGK is an enzyme of 467 residues with two domains, which include several $\beta$-strands, thus the presence of multiple intermediates is highly probable. The mechanical intermediate 1 was present in all the conditions explored, whereas intermediate 1* was observed predominantly when substrates are bound to the enzyme; however, the highest stabilization is attained only in the E·A·B complex. Considering its fold and topology, several $\beta$-strands could be related to the mechanical clamp formation. Also, taking into account that the binding of both substrates changes the mechanical stability of intermediates 1 and 1*, these should be in the neighborhood of the active site. Analysis of the holo-TlGK crystal structure reveals that the longest parallel $\beta$-structure present in the enzyme is located in the small domain between the $\beta$-strands 2 and 8 (residues Asn40 and Pro190) (Supporting Information Figures S3 and S4).[34] Therefore, considering that intermediate 1 should be located at the end of the unfolding pathway, capturing the last 60 nm of the protein—or 150 residues (Table 2), the structure between $\beta$-strand 2 and $\beta$-strand 8 (150 residues) is a good candidate for the mechanical clamp present in the intermediate 1 (Supporting Information Figure S3B). On the other hand, assigning a specific structure to the mechanical intermediate 1*, which is reached when

only a few amino acids are pulled from the enzyme, is more complicated. Considering that both N- and C-termini are located in the large domain of TlGK, it is very likely that the mechanical clamp present in the intermediate 1* is formed by an arrangement of $\beta$-strands of this domain. A combination of parallel $\beta$-strands from the large domain, $\beta$-strands $\beta 1 - \beta 10 - \beta 11 - \beta 12 - \beta 13$ (~166 residues), have an extension of 66.4 nm (Supporting Information Figure S3C), very close to the extension of 66−68 nm observed in the $\Delta L_{C1*}$ (Table 4). However, if we consider that the full length of the enzyme is ~190 nm (187 or 196 nm considering extension of linkers; see Methods) to reach intermediates 1 and 1*, a segment of the enzyme should already be unfolded. Approximately, 70 nm of the enzyme should experience unfolding before intermediates 1 and 1*, which are not detected during the mechanical unfolding with a distinguishable signature in force. The remaining structure not considered in the intermediates 1 and 1* includes $\alpha 1$ (residues 1−32) and the C-terminal $\alpha/\beta$ structure between $\beta 14$ and $\alpha 17$ (residues 306−467) (Supporting Information Figure S2D). Together both structures have an extension of around 77 nm (Supporting Information Figure S3D). It is known that antiparallel $\beta$-sheets and $\alpha$-helices can be unfolded with less force than parallels $\beta$-sheet, with forces below 20 pN.[49] Therefore, it is likely that the $\alpha 1$ and $\alpha/\beta$ structure $\alpha 17/\beta 14$ unfold at forces below our force resolution limit, which is around 20−30 pN using this force−extension protocol.

Inspection in the crystal structures of TlGK reveals that both intermediates present residues involved in the stabilization of the substrates (Supporting Information Figure S4). Thus, it is possible to think that the binding of the complex Mg·ADP$^-$ and D-glucose can be sensed by these intermediates. Additionally, the $\alpha 1$ and $\alpha/\beta$ structure $\alpha 17/\beta 14$ are not involved in the binding of D-glucose, and only Val440 (included in $\alpha 17/\beta 14$ structure), which participates in the binding of Mg·ADP$^-$,[31] is removed during the mechanical unfolding. Therefore, the location of the substrate binding sites within the mechanical clamp explains the increase in mechanical stability of the intermediates when the unfolding is assayed in the presence of the substrates.

## CONCLUSIONS

We have explored the strength of single-molecule force spectroscopy (SMFS) as a tool to assess the substrate-induced conformational changes experienced by the thermophilic enzyme TlGK in order to reach the catalytic ternary complex. Our results not only provide information about the mechanical stabilization induced by the substrates on TlGK but also embody the use of SMFS to identify its sequential order of binding to the active site. The combination of protein engineering and SMFS should be included among the techniques used to identify kinetic mechanism of enzymes or in the case of protein−protein and protein−ligand interactions. An SMFS-based approach is desirable because it requires very small amounts of enzyme and reagents, and multiple conditions can be explored easily, overcoming the drawbacks of traditional techniques. Additionally, our experimental assay can be applied to different systems and opens new alternatives to study protein−ligand interactions in solution, especially useful for the identification of modulators of enzyme activities with medical relevance and for the discovery of new allosteric effectors. In light of the new HaloTag technology for covalent anchoring,[50] which increases the pickup rate, fingerprint with full length, and the time that the molecule is attached to the surface/tip, the effect of the substrates and inhibitors in the unfolding and refolding of enzymes can be now studied in the same molecule.

## METHODS

**Purification of the Polyprotein (I27)₂-TlGK-(I27)₂.** The TlGK polyprotein was engineered using the same strategy reported previously.[35] The cDNA coding for TlGK was kindly provided by Dr. Takayoshi Wakagi (University of Tokyo). Restriction sites *Bam*HI, *Bgl*II, and *Kpn*I were added, flanking the construct following a method described elsewhere.[38] The TlGK gene normally has a *Bgl*II restriction site that was removed and replaced by a silent mutation using GeneTailor site-directed mutagenesis (Invitrogen). The final construct (I27)₂-TlGK-(I27)₂ was cloned into the expression vector pQE80L (Qiagen) by using the *Bam*HI and *Kpn*I restriction sites.

The full-length polyprotein comprises 847 amino acid residues corresponding to four copies of I27 (89 residues each repeat), one copy of TlGK (467 residues), 13 extra amino acids in the N-terminus including a His-tag, two residues in the C-terminus, and two residues between each module except between the TlGK and the next C-terminal I27 module, where the linker is composed of three residues (nine linker residues in total).

The polyprotein was expressed in *Escherichia coli* BLR (DE3) pLysS cells at 25 °C. When the OD$_{600nm}$ of the culture reached 0.7, protein expression was induced by 1 mM IPTG overnight. The cells were lysed by sonication and French press in sodium phosphate pH 7.0, 300 mM NaCl. The soluble fraction was loaded onto a Talon affinity chromatography column (Clontech). The fractions containing the polyprotein were pooled and run on a Superdex-200 size-exclusion chromatography column (GE Healthcare), eluting with 10 mM Hepes, pH 7.2, 150 mM NaCl, 1 mM EDTA. The fractions were analyzed by SDS-PAGE to ensure a homogeneous purification.

**Enzyme Kinetics Experiments.** We followed the activity of the TlGK by monitoring spectrophotometrically NAD$^+$ reduction at 340 nm coupled with the oxidation of D-glucose-6-phosphate. The enzyme activity assays were carried out as described previously.[31] Briefly, each measurement was performed in 1 mL of buffer with 25 mM Hepes, pH 7.8, 0.5 mM NAD$^+$, 1 mM free Mg$^{2+}$, and five units of D-glucose-6-phosphate dehydrogenase. For the Mg·ADP$^-$ and D-glucose saturation curves, the concentration of the cosubstrate was fixed to 1 mM. Kinetics parameters, maximal velocity ($V_{max}$), and the apparent Michaelis constants for both substrates ($K_M$) were calculated by

fitting initial velocities to the Michaelis–Menten model:

$$v_0 = \frac{v_{max} \cdot S}{K_M + S} \tag{1}$$

**Single-Molecule Force Spectroscopy.** The experiments were performed using a custom-built atomic force microscope (AFM),[51] following the procedure described in Popa et al.,[39] with a few modifications. Briefly, 5–10 $\mu$L of polyprotein sample from a ~0.1 mg·mL$^{-1}$ stock solution was left to adsorb on a gold-coated glass coverslip. The fluid cell, mounted on top of the AFM, was sealed after 10–15 min of incubation to prevent full evaporation of the sample. MLCT cantilevers (Bruker) were calibrated using the equipartition theorem.[52] For our experiments, the spring constants were between 14 and 20 pN·nm$^{-1}$. In the force–extension experiments, a pulling velocity of 400 nm·s$^{-1}$ was used. Single-molecule tethers were formed by pushing the cantilever against the polyprotein-containing surface for 0.5–1.0 s. All of the measurements were made in 10 mM Hepes, pH 7.2, 150 mM NaCl. For assays in the presence of both substrates, 10 mM D-glucose, 7 mM Mg$^{2+}$, and 5 mM ADP$\beta$S$^{3-}$ (a nonhydrolyzable analogue of ADP$^{3-}$) were added. For experiments in the presence of only Mg·ADP$^-$, 7 mM Mg$^{2+}$ and 5 mM ADP$^{3-}$ were added, whereas for only D-glucose assays, 10 mM D-glucose was added to the solution. For the experiments in the presence of the inhibitor Mg·GDP$^-$, 11 mM Mg$^{2+}$ and 10 mM GDP$^{3-}$ were used. The molecule adenosine-5'-diphosphoglucose (ADP-GLC$^{2-}$), which has the nucleotide and sugar joined via a 5' glycosidic linkage, was used as an analogue to the ternary complex E·A·B. For this, 10 mM of ADP-GLC$^{2-}$ supplemented with 11 mM Mg$^{2+}$ was used. All of the experiments were done at room temperature.

**Data Analysis.** Only traces with at least three events of I27 unfolding were considered for analysis; this was to ensure that the traces analyzed included the full unfolding of the enzyme TlGK. We used the elasticity polymer model worm-like chain to calculate the extension of the unfolding events.[53,54] From the peak of these unfolding events, we calculated the unfolding force for I27 and TlGK. We fitted Gaussian distribution to the unfolding extensions and unfolding force histograms. The forces experienced for the mechanical intermediates present in TlGK ($\Delta L_{C1}$ and $\Delta L_{C1*}$) and in I27 modules ($\Delta L_{C\ I27}$) were analyzed using one-way ANOVA considering individual unfolding force events. Bonferroni post-test was used to determine the significant differences between the pairs compared. The populations were considered significantly different when $P < 0.05$.

*Conflict of Interest:* The authors declare no competing financial interest.

*Supporting Information Available:* Histograms showing the unfolding forces of the I27 module in the absence and presence of substrates is presented in Figure S1. Individual statistical error of the data collected for each condition has been included in Table S1. Binding experiments, in the absence and presence of the substrates, are presented in Figure S2. Additionally, possible locations of the mechanical intermediates and mechanical clamps present in $\Delta L_{C1}$ and $\Delta L_{C1*}$ are shown in Figures S3 and S4. This material is available free of charge via the Internet at http://pubs.acs.org.

## REFERENCES AND NOTES

1. Bakan, A.; Bahar, I. The Intrinsic Dynamics of Enzymes Plays a Dominant Role in Determining the Structural Changes Induced upon Inhibitor Binding. *Proc. Natl. Acad. Sci. U.S.A.* **2009**, *106*, 14349–14354.
2. Sigrell, J. A.; Cameron, A. D.; Mowbray, S. L. Induced Fit on Sugar Binding Activates Ribokinase. *J. Mol. Biol.* **1999**, *290*, 1009–1018.
3. Street, T. O.; Lavery, L. A.; Agard, D. A. Substrate Binding Drives Large-Scale Conformational Changes in the Hsp90 Molecular Chaperone. *Mol. Cell* **2011**, *42*, 96–105.
4. Zerrad, L.; Merli, A.; Schroder, G. F.; Varga, A.; Graczer, E.; Pernot, P.; Round, A.; Vas, M.; Bowler, M. W. A Spring-Loaded Release Mechanism Regulates Domain Movement and Catalysis in Phosphoglycerate Kinase. *J. Biol. Chem.* **2011**, *286*, 14040–14048.
5. Cabrera, R.; Fischer, H.; Trapani, S.; Craievich, A. F.; Garratt, R. C.; Guixe, V.; Babul, J. Domain Motions and Quaternary Packing of Phosphofructokinase-2 from *Escherichia coli* Studied by Small Angle X-ray Scattering and Homology Modeling. *J. Biol. Chem.* **2003**, *278*, 12913–12919.
6. Davulcu, O.; Flynn, P. F.; Chapman, M. S.; Skalicky, J. J. Intrinsic Domain and Loop Dynamics Commensurate with Catalytic Turnover in an Induced-Fit Enzyme. *Structure* **2009**, *17*, 1356–1367.
7. Sullivan, S. M.; Holyoak, T. Enzymes with Lid-Gated Active Sites Must Operate by an Induced Fit Mechanism Instead of Conformational Selection. *Proc. Natl. Acad. Sci. U.S.A.* **2008**, *105*, 13829–13834.
8. Tsuge, H.; Sakuraba, H.; Kobe, T.; Kujime, A.; Katunuma, N.; Ohshima, T. Crystal Structure of the ADP-Dependent Glucokinase from *Pyrococcus horikoshii* at 2.0-Å Resolution: A Large Conformational Change in ADP-Dependent Glucokinase. *Protein Sci.* **2002**, *11*, 2456–2463.
9. Qasba, P. K.; Ramakrishnan, B.; Boeggeman, E. Substrate-Induced Conformational Changes in Glycosyltransferases. *Trends Biochem. Sci.* **2005**, *30*, 53–62.
10. Ito, S.; Fushinobu, S.; Jeong, J. J.; Yoshioka, I.; Koga, S.; Shoun, H.; Wakagi, T. Crystal Structure of an ADP-Dependent Glucokinase from Pyrococcus Furiosus: Implications for a Sugar-Induced Conformational Change in ADP-Dependent Kinase. *J. Mol. Biol.* **2003**, *331*, 871–883.
11. Cleland, W. W. The Kinetics of Enzyme-Catalyzed Reactions with Two or More Substrates or Products. I. Nomenclature and Rate Equations. *Biochim. Biophys. Acta* **1963**, *67*, 104–137.
12. Cleland, W. W. The Kinetics of Enzyme-Catalyzed Reactions with Two or More Substrates or Products. II. Inhibition: Nomenclature and Theory. *Biochim. Biophys. Acta* **1963**, *67*, 173–187.
13. Cleland, W. W. The Kinetics of Enzyme-Catalyzed Reactions with Two or More Substrates or Products. III. Prediction of Initial Velocity and Inhibition Patterns by Inspection. *Biochim. Biophys. Acta* **1963**, *67*, 188–196.
14. Segel, I. H. *Enzyme Kinetics: Behavior and Analysis of Rapid Equilibrium and Steady State Enzyme Systems*, Wiley Classics Library; Wiley: New York, 1993; pp 560–590.
15. Cleland, W. W. Steady State Kinetics. In *The Enzymes*, 3rd ed.; Boyer, P. D., Ed.; Academic Press: New York, 1970; pp 1–65.
16. Cleland, W. W. Substrate Inhibition. *Methods Enzymol.* **1979**, *63*, 500–513.
17. McClure, W. R. A Kinetic Analysis of Coupled Enzyme Assays. *Biochemistry* **1969**, *8*, 2782–2786.
18. Storer, A. C.; Cornish-Bowden, A. The Kinetics of Coupled Enzyme Reactions. Applications to the Assay of Glucokinase, with Glucose 6-Phosphate Dehydrogenase as Coupling Enzyme. *Biochem. J.* **1974**, *141*, 205–209.
19. Cornish-Bowden, A. *Fundamentals of Enzyme Kinetics*, 3rd ed.; Portland Press: London, 2004; pp 71–90.
20. Bertz, M.; Rief, M. Ligand Binding Mechanics of Maltose Binding Protein. *J. Mol. Biol.* **2009**, *393*, 1097–1105.
21. del Rio, A.; Perez-Jimenez, R.; Liu, R.; Roca-Cusachs, P.; Fernandez, J. M.; Sheetz, M. P. Stretching Single Talin Rod Molecules Activates Vinculin Binding. *Science* **2009**, *323*, 638–641.

22. Kawamura, S.; Gerstung, M.; Colozo, A. T.; Helenius, J.; Maeda, A.; Beerenwinkel, N.; Park, P. S.; Muller, D. J. Kinetic, Energetic, and Mechanical Differences between Dark-State Rhodopsin and Opsin. *Structure* **2013**, *21*, 426–437.

23. Ainavarapu, S. R.; Li, L.; Badilla, C. L.; Fernandez, J. M. Ligand Binding Modulates the Mechanical Stability of Dihydrofolate Reductase. *Biophys. J.* **2005**, *89*, 3337–3344.

24. Junker, J. P.; Ziegler, F.; Rief, M. Ligand-Dependent Equilibrium Fluctuations of Single Calmodulin Molecules. *Science* **2009**, *323*, 633–637.

25. Wang, C. C.; Tsong, T. Y.; Hsu, Y. H.; Marszalek, P. E. Inhibitor Binding Increases the Mechanical Stability of Staphylococcal Nuclease. *Biophys. J.* **2011**, *100*, 1094–1099.

26. Junker, J. P.; Hell, K.; Schlierf, M.; Neupert, W.; Rief, M. Influence of Substrate Binding on the Mechanical Stability of Mouse Dihydrofolate Reductase. *Biophys. J.* **2005**, *89*, L46–48.

27. Cao, Y.; Yoo, T.; Li, H. Single Molecule Force Spectroscopy Reveals Engineered Metal Chelation Is a General Approach To Enhance Mechanical Stability of Proteins. *Proc. Natl. Acad. Sci. U.S.A.* **2008**, *105*, 11152–11157.

28. Muller, D. J. AFM: A Nanotool in Membrane Biology. *Biochemistry* **2008**, *47*, 7986–7998.

29. Puchner, E. M.; Gaub, H. E. Force and Function: Probing Proteins with AFM-Based Force Spectroscopy. *Curr. Opin. Struct. Biol.* **2009**, *19*, 605–614.

30. Kotamarthi, H. C.; Sharma, R.; Narayan, S.; Ray, S.; Ainavarapu, S. R. Multiple Unfolding Pathways of Leucine Binding Protein (LBP) Probed by Single-Molecule Force Spectroscopy (SMFS). *J. Am. Chem. Soc.* **2013**, *135*, 14768–14774.

31. Rivas-Pardo, J. A.; Herrera-Morande, A.; Castro-Fernandez, V.; Fernandez, F. J.; Vega, M. C.; Guixe, V. Crystal Structure, SAXS and Kinetic Mechanism of Hyperthermophilic ADP-Dependent Glucokinase from *Thermococcus litoralis* Reveal a Conserved Mechanism for Catalysis. *PLoS One* **2013**, *8*, e66687.

32. Sakuraba, H.; Goda, S.; Ohshima, T. Unique Sugar Metabolism and Novel Enzymes of Hyperthermophilic Archaea. *Chem. Rec.* **2004**, *3*, 281–287.

33. Wetlaufer, D. B. Nucleation, Rapid Folding, and Globular Intrachain Regions in Proteins. *Proc. Natl. Acad. Sci. U.S.A.* **1973**, *70*, 697–701.

34. Ito, S.; Fushinobu, S.; Yoshioka, I.; Koga, S.; Matsuzawa, H.; Wakagi, T. Structural Basis for the ADP-Specificity of a Novel Glucokinase from a Hyperthermophilic Archaeon. *Structure* **2001**, *9*, 205–214.

35. Perez-Jimenez, R.; Garcia-Manyes, S.; Ainavarapu, S. R.; Fernandez, J. M. Mechanical Unfolding Pathways of the Enhanced Yellow Fluorescent Protein Revealed by Single Molecule Force Spectroscopy. *J. Biol. Chem.* **2006**, *281*, 40010–40014.

36. Alegre-Cebollada, J.; Badilla, C. L.; Fernandez, J. M. Isopeptide Bonds Block the Mechanical Extension of Pili in Pathogenic *Streptococcus pyogenes*. *J. Biol. Chem.* **2010**, *285*, 11235–11242.

37. Ainavarapu, S. R.; Brujic, J.; Huang, H. H.; Wiita, A. P.; Lu, H.; Li, L.; Walther, K. A.; Carrion-Vazquez, M.; Li, H.; Fernandez, J. M. Contour Length and Refolding Rate of a Small Protein Controlled by Engineered Disulfide Bonds. *Biophys. J.* **2007**, *92*, 225–233.

38. Carrion-Vazquez, M.; Oberhauser, A. F.; Fowler, S. B.; Marszalek, P. E.; Broedel, S. E.; Clarke, J.; Fernandez, J. M. Mechanical and Chemical Unfolding of a Single Protein: A Comparison. *Proc. Natl. Acad. Sci. U.S.A.* **1999**, *96*, 3694–3699.

39. Popa, I.; Kosuri, P.; Alegre-Cebollada, J.; Garcia-Manyes, S.; Fernandez, J. M. Force Dependency of Biochemical Reactions Measured by Single-Molecule Force-Clamp Spectroscopy. *Nat. Protoc.* **2013**, *8*, 1261–1276.

40. Holmgren, A.; Bjornstedt, M. Thioredoxin and Thioredoxin Reductase. *Methods Enzymol.* **1995**, *252*, 199–208.

41. Kadokura, H.; Beckwith, J. Mechanisms of Oxidative Protein Folding in the Bacterial Cell Envelope. *Antioxid. Redox Signal.* **2010**, *13*, 1231–1246.

42. Koshland, D. E. Application of a Theory of Enzyme Specificity to Protein Synthesis. *Proc. Natl. Acad. Sci. U.S.A.* **1958**, *44*, 98–104.

43. Berger, C.; Weber-Bornhauser, S.; Eggenberger, J.; Hanes, J.; Pluckthun, A.; Bosshard, H. R. Antigen Recognition by Conformational Selection. *FEBS Lett.* **1999**, *450*, 149–153.

44. Kumar, S.; Ma, B.; Tsai, C. J.; Sinha, N.; Nussinov, R. Folding and Binding Cascades: Dynamic Landscapes and Population Shifts. *Protein Sci.* **2000**, *9*, 10–19.

45. Aggarwal, V.; Kulothungan, S. R.; Balamurali, M. M.; Saranya, S. R.; Varadarajan, R.; Ainavarapu, S. R. Ligand-Modulated Parallel Mechanical Unfolding Pathways of Maltose-Binding Proteins. *J. Biol. Chem.* **2011**, *286*, 28056–28065.

46. Puchner, E. M.; Alexandrovich, A.; Kho, A. L.; Hensen, U.; Schafer, L. V.; Brandmeier, B.; Grater, F.; Grubmuller, H.; Gaub, H. E.; Gautel, M. Mechanoenzymatics of Titin Kinase. *Proc. Natl. Acad. Sci. U.S.A.* **2008**, *105*, 13385–13390.

47. Cao, Y.; Balamurali, M. M.; Sharma, D.; Li, H. A Functional Single-Molecule Binding Assay *via* Force Spectroscopy. *Proc. Natl. Acad. Sci. U.S.A.* **2007**, *104*, 15677–15681.

48. Giganti, D.; Alegre-Cebollada, J.; Urresti, S.; Albesa-Jove, D.; Rodrigo-Unzueta, A.; Comino, N.; Kachala, M.; Lopez-Fernandez, S.; Svergun, D. I.; Fernandez, J. M.; Guerin, M. E. Conformational Plasticity of the Essential Membrane-Associated Mannosyltransferase Pima from Mycobacteria. *J. Biol. Chem.* **2013**, *288*, 29797–29808.

49. West, D. K.; Brockwell, D. J.; Olmsted, P. D.; Radford, S. E.; Paci, E. Mechanical Resistance of Proteins Explained Using Simple Molecular Models. *Biophys. J.* **2006**, *90*, 287–297.

50. Popa, I.; Berkovich, R.; Alegre-Cebollada, J.; Badilla, C. L.; Rivas-Pardo, J. A.; Taniguchi, Y.; Kawakami, M.; Fernandez, J. M. Nanomechanics of Halotag Tethers. *J. Am. Chem. Soc.* **2013**, *135*, 12762–12771.

51. Oberhauser, A. F.; Marszalek, P. E.; Erickson, H. P.; Fernandez, J. M. The Molecular Elasticity of the Extracellular Matrix Protein Tenascin. *Nature* **1998**, *393*, 181–185.

52. Florin, E. L.; Rief, M.; Lehmann, H.; Ludwig, M.; Dornmair, C.; Moy, V. T.; Gaub, H. E. Sensing Specific Molecular-Interactions with the Atomic-Force Microscope. *Biosens. Bioelectron.* **1995**, *10*, 895–901.

53. Marko, J. F.; Siggia, E. D. Stretching DNA. *Macromolecules* **1995**, *28*, 8759–8770.

54. Rief, M.; Gautel, M.; Oesterhelt, F.; Fernandez, J. M.; Gaub, H. E. Reversible Unfolding of Individual Titin Immunoglobulin Domains by AFM. *Science* **1997**, *276*, 1109–1112.